ISSN 1232-3829
tts
10/2013
Technika Transportu Szynowego koleje ▪ tramwaje ▪ metro

LUFT Mirosław, SZYCHTA Elżbieta, PIETRUSZCZAK Daniel

LABORATORY INVESTIGATIONS OF DYNAMIC PROPERTIES OF FRACTIONAL-ORDER ACCELEROMETERS

Abstract

The paper shows possibilities of using fractional calculus in dynamic measurements. It describes a laboratory measurement system for investigating dynamic properties of measuring transducers. Transducer's dynamics are identified by the ARX method. Properties of the examined transducers of integral and fractional orders are compared. The authors indicate the fractional calculus advantages from the point of view of their dynamics description.

INTRODUCTION

The recent dynamic development of research into application of the fractional calculus to analysis of dynamic systems [1], [5] has encouraged the authors to attempt its application to analysis and modelling of measuring transducers, described by means of the 'classic' mathematical analysis so far .

Transducers measuring accelerations (accelerometers) are tested, treated as a representative group of measuring transducers. In the classic notation, accelerometers are described with second-order differential equations, like many other groups of measuring transducers, such as: RLC, mechanical vibrating systems, displacement measurement sensors, systems including tensometric and piezoelectric transducers. In addition, linear transducers of higher than second orders, when in transitional states, behave in ways similar to second-order linear transducers.

The aim of this paper is to show how models of accelerometers based on the fractional calculus notation convey their dynamic behaviour in comparison to models represented by differential equations of integer orders and in comparison to processing characteristics of their real counterparts.

1. MATHEMATICAL MODEL OF MEASURING TRANSDUCER (ACCELEROMETERS)

A measuring transducer comprising three types of elements characteristic for linear systems, i.e.: elements storing kinetic energy, elements storing potential energy and elements causing energy losses, are referred to as second-order measuring transducers.

Simulation and laboratory testing of a second-order transducer measuring accelerations (accelerometer) has been tested in this paper, treated as a representative group of measuring transducers (Fig. 1.).

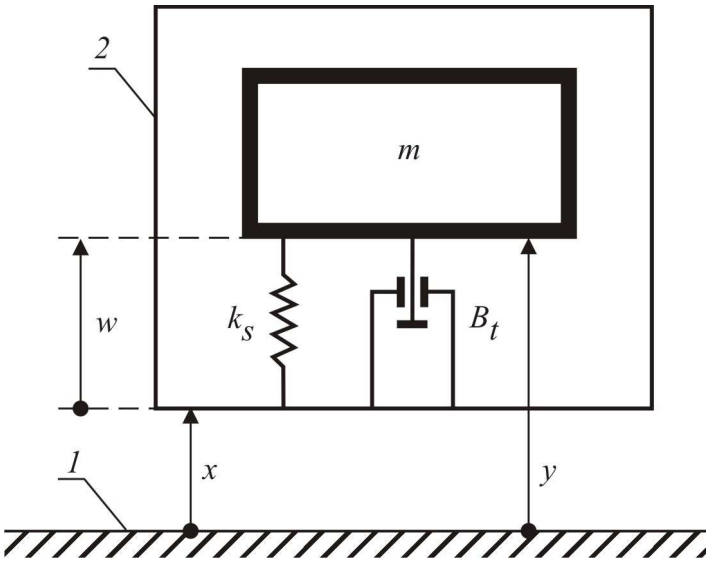

Fig. 1. Kinetic diagram of an accelerometer: m – seismic mass, k_s – spring constant, B_t – damping coefficient, x – distance relative to a fixed system of coordinates, y – distance of a vibrating mass relative to a fixed system of coordinates, w – distance of a vibrating mass relative to a vibrating object

Source: [2]

A differential equation describing the absolute motion of a second-order measuring transducer's (accelerometer's) seismic mass can be expressed as:

$$\frac{d^2}{dt^2}y(t) + 2\zeta\omega_0\frac{d}{dt}y(t) + \omega_0^2 y(t) = \omega_0^2 x(t) + 2\zeta\omega_0\frac{d}{dt}x(t) \tag{1}$$

where: $\omega_0 = \sqrt{\frac{k_s}{m}}$ - circular frequency of free vibrations, $\zeta = \frac{B_t}{2\sqrt{k_s m}}$ - degree of damping

and $k = \frac{1}{k_s}$ - amplification factor.

Considering the motion of the vibrating mass relative to the vibrating object (Fig. 1):

$$w(t) = y(t) - x(t) \tag{2}$$

$$\frac{d^2}{dt^2}w(t) + 2\zeta\omega_0\frac{d}{dt}w(t) + \omega_0^2 w(t) = -\frac{d^2}{dt^2}x(t) \tag{3}$$

Depending on selection of k_S, m and B_t, a transducer can serve to measure displacements as a vibrometer assuming low k_S and B_t and high m (Fig. 3), or acceleration as an accelerometer assuming a high k_S, low m and B_t (Fig. 2). This corresponds to two cases: where the frequency of the object's vibrations is much lower than circular frequency of free vibrations: $\omega_m << \omega_0$ – accelerometer (Fig. 2), or where the frequency of the object's vibrations is much greater than the circular frequency of free vibrations: $\omega_m >> \omega_0$ – vibrometer (Fig. 3).

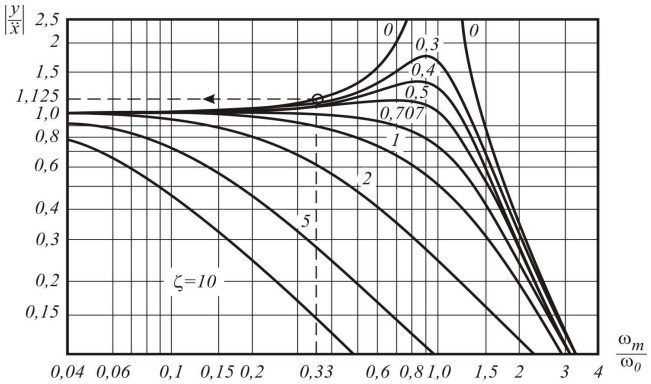

Fig. 2. Characteristic of the equation of measuring transducer's seismic mass motion for $\omega_m << \omega_0$:
ω_m – measured frequencies, ω_0 – circular frequency of free vibrations, y – real mass displacements, $\ddot{x}$ – displacement of the housing
Source: [6]

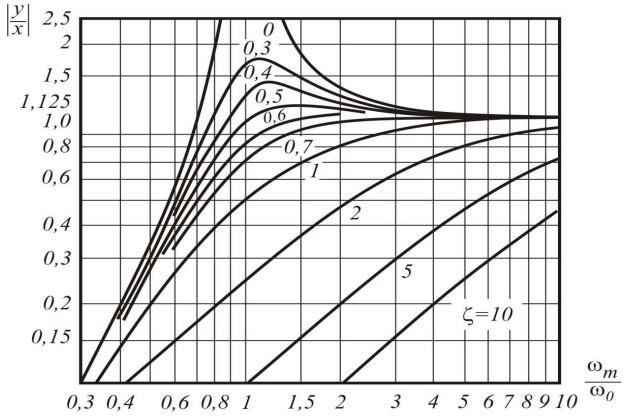

Fig. 3. Characteristic of the equation of measuring transducer's seismic mass motion for: $\omega_m >> \omega_0$:
ω_m – measured frequencies, ω_0 – circular frequency of free vibrations, y – real mass displacements, x – displacement of the housing
Source: [6]

In practical vibration measurements, acceleration-measuring transducers, the so-called accelerometers, are employed.
For purposes of simulation testing, a measuring transducer was assumed of a frequency $f = 350Hz$, that is, circular frequency of free vibrations $\omega_0 = 2200\frac{rad}{s}$ and degree of damping $\zeta = 0.2$. Dynamics of such a transducer, characterised by means of a 2nd-order differential equation (1), are described by operator transmittance:

$$G(s) = \frac{1}{s^2 + 880s + 4.84 \cdot 10^6} \tag{4}$$

Fig. 4 shows step response of a transducer with an operator transmittance (4). The amplitude value for the step response stabilizes after $0.01\,\mathrm{s}$ in the simulations. Fig. 5 illustrates logarithm, amplitude and phase frequency characteristics of a measuring transducer with operator transmittance (4).

Simulation testing of the measuring transducer (4) was conducted in an operation band without amplitude distortions. The band is part of the amplitude characteristic's linear range from $10\,\mathrm{Hz}$ to above $10^2\,\mathrm{Hz}$. Fig. 7 shows the transducer's response to a sinusoid input of 100Hz.

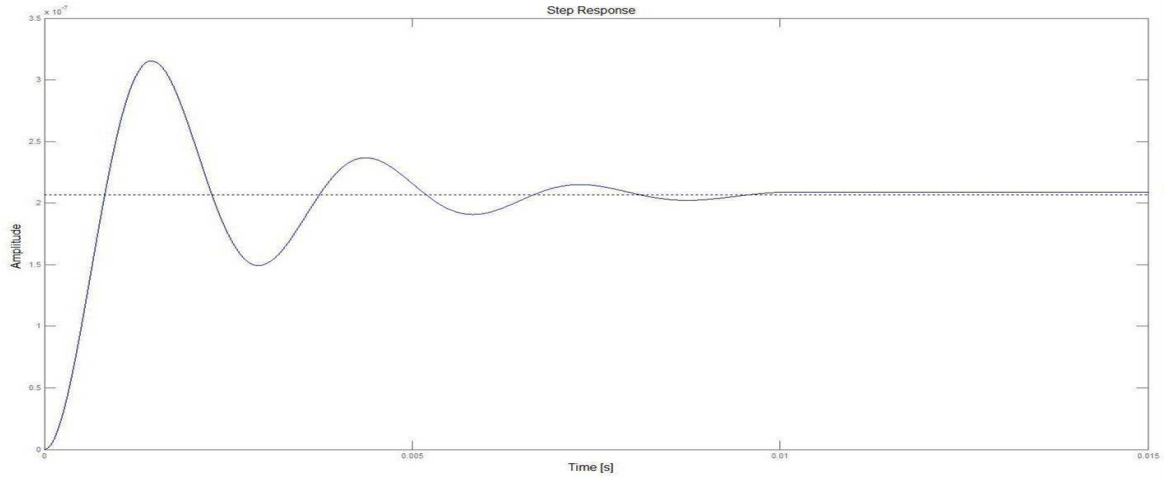

Fig. 4. Step response of measuring transducer (4)
Source: [6]

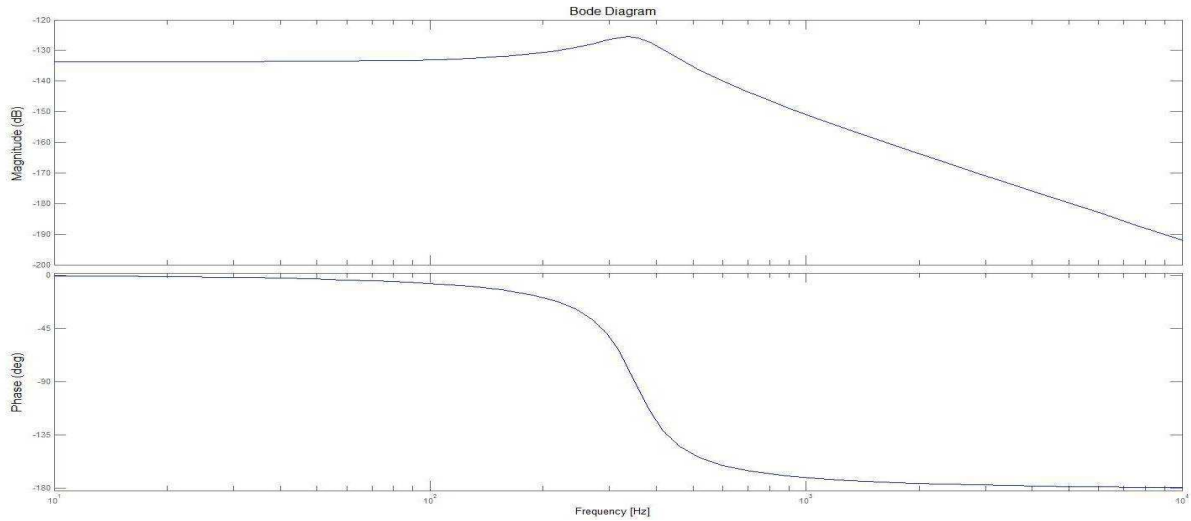

Fig. 5. Amplitude and phase diagrams of measuring transducer (4)
Source: [6]

2. FRACTIONAL FORMULATION OF THE MEASURING TRANSDUCER MODEL

The equation (1), describing the measuring transducer, can be expressed as a difference equation:

$$a_2 w_k + a_1 w_{k-1} + a_0 w_{k-2} = b_2 x_k + b_1 x_{k-1} + a_0 x_{k-2} \tag{5}$$

or:

$$\begin{bmatrix} a_2 & a_1 & a_0 \end{bmatrix} \begin{bmatrix} w_k \\ w_{k-1} \\ w_{k-2} \end{bmatrix} = \begin{bmatrix} b_2 & b_1 & b_0 \end{bmatrix} \begin{bmatrix} x_k \\ x_{k-1} \\ x_{k-2} \end{bmatrix}. \tag{6}$$

Equation (5) can have the following derivative-integral expression:

$$A_2 \Delta_k{}^{(2)} w_k + A_1 \Delta_{k-1}{}^{(1)} + A_0 w_{k-2} = B_2 \Delta_k{}^{(2)} w_k + B_1 \Delta_k{}^{(1)} x_{k-1} + B_0 w_{k-2} \tag{7}$$

where $\Delta_k^{(n)}$ is the discrete function's reverse difference, defined as:

$$\Delta_k^{(n)} f(k) = \sum_{j=0}^{k} a_j^{(n)} f(k-j) \tag{8}$$

for: $n = 1, 2, \ldots.$

When (8) is taken into account, (6) has the form:

$$\begin{bmatrix} a_2 & -a_1 - 2a_0 & a_2 + a_1 + a_0 \end{bmatrix} \begin{bmatrix} \Delta_k^{(2)} w_k \\ \Delta_k^{(1)} w_k \\ \Delta_k^{(0)} w_k \end{bmatrix} = \begin{bmatrix} b_0 & -b_1 - 2b_0 & b_2 + b_1 + b_0 \end{bmatrix} \begin{bmatrix} \Delta_k^{(2)} x_k \\ \Delta_k^{(1)} x_k \\ \Delta_k^{(0)} x_k \end{bmatrix} \tag{9}$$

where: $A_2 = a_2, A_1 = -a_1 - 2a_0, A_0 = a_2 + a_1 + a_0$ and: $B_2 = b_0 + b_1 + b_2, B_1 = -b_1 - 2b_0, B_0 = b_0$.

Using the above method has received three models describing the measuring transducer:

- classic model (transfer function of measuring transducer model) described with operator transmittance (10):

$$G(s) = \frac{1}{s^2 + 880s + 4.84 \cdot 10^6} \tag{10}$$

Operation of a transducer described with the equation was simulated for appropriately selected parameters: natural angular frequency and degree of damping. Dynamics of the measuring transducer described by operator transmittance (4) were adopted as follows:

- classic discrete model (discrete transfer function of measuring transducer model), derived from the operator transmittance model (10), described by means of discrete transmittance (11):

$$G(z) = \frac{1.667 \cdot 10^{-15} z^2 + 6.666 \cdot 10^{-15} z + 1.667 \cdot 10^{-15}}{z^2 - 2z + 0.999}. \tag{11}$$

- Response of a continuous object to a discrete input depends not only on values of this signal at a discrete moments of time but also on sampling time and the extrapolator used.

MATLAB&Simulink programming environment provides a number of criteria which can be employed to define a discrete equivalent of the continuous object. ZOH (Zero-Order-Hold) is the default and most commonly used extrapolator. This corresponds to extrapolation with a zero-order polynomial (staircase function). Thus, the classic discrete model (11) was obtained by discretising the classic model (10), the Zero-Order-Hold model with a sampling time: $T_p = 10^{-7}$ s, for which Nyquist theorem of sampling frequency selection holds true.

- discrete model (discrete transfer function of fractional transducer model) is expressed with derivative integrals and described by discrete transmittance:

$$G(z) = \frac{z^2}{1 \cdot 10^{14} z^2 - 2 \cdot 10^{14} z + 1 \cdot 10^{14}}. \tag{12}$$

The discrete transmittance (12) is produced by implementation of the method of determining expression from (5) to (9) of the measuring transducer in MATLAB&Simulink. Reverse differences of the discrete function $\Delta_k^{(n)} f(k)$ were determined according to (8), which produced:

$$A_2 = a_2 = 1, A_1 = -a_1 - 2a_0 = 0, A_0 = a_2 + a_1 + a_0 = 0 \tag{13}$$

where:

$$B_2 = b_0 + b_1 + b_2 = 10^{14}, B_1 = -b_1 - 2b_0 = -2 \cdot 10^{14}, B_0 = b_0 = 10^{14}. \tag{14}$$

Models' responses were tested in the programming environment MATLAB&Simulink. Responses of all measuring transducer models to the input sinusoid 100Hz signal are illustrated in Fig. 7. Model signals are not phase shifted in relation to the input signal and have a different amplitude. It can be noted that the model described by means of the discrete transmittance (12) correctly reproduces values of the input signal amplitude, like the model of transmittance (11). It can be noted in Bode frequency diagrams (Fig. 9) that the measuring transducer model determined by the derivative-integral method presents the dynamics of the classically determined model (the diagrams of the models coincide).

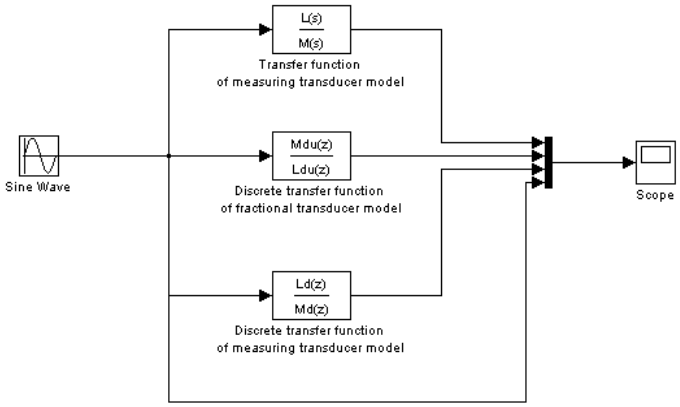

Fig. 6. Simulation diagram of the system comparing measuring transducer models: Transfer function of measuring transducer model – transducer model of operator transmittance (10), Discrete transfer function of measuring transducer model – discrete transducer model of transmittance (11), Discrete transfer function of fractional transducer model – fractional discrete model (12)
Source: [3]

Measuring transducer models (11) and (12) have only been subject to simulation testing and do not fully represent real models. The simulations indicate that the fractional model (12) exhibits the same dynamics as the classic model.

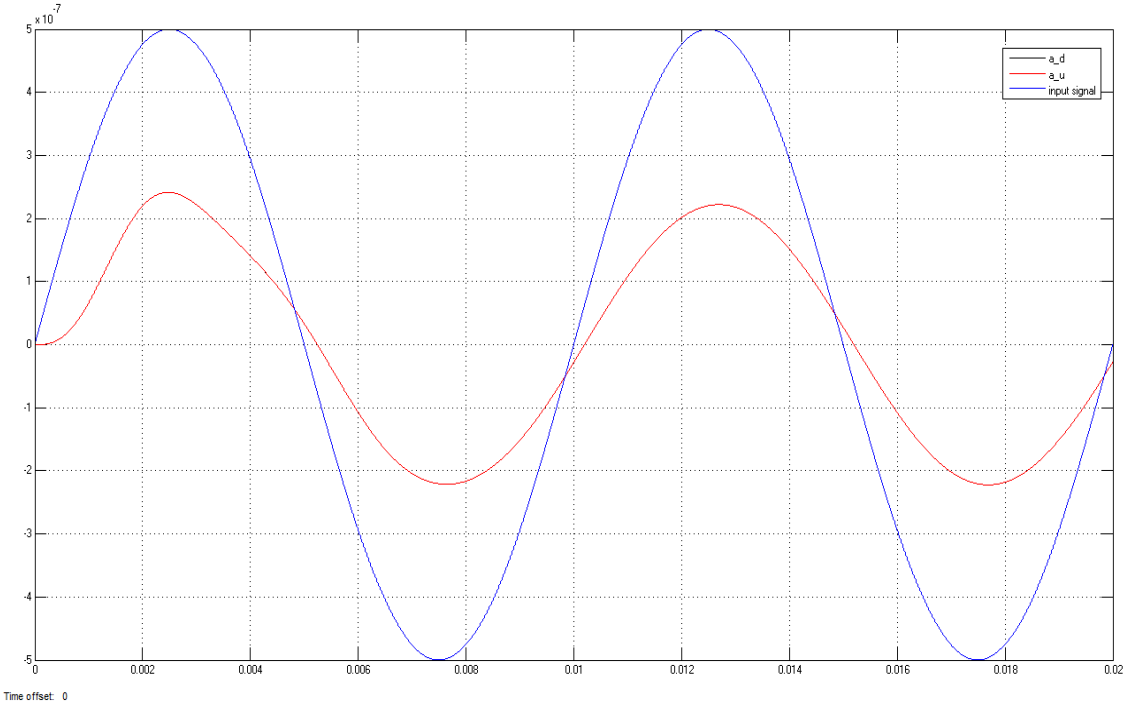

Fig. 7. Comparison of responses by measuring transducer models (11) and (12) to sinusoid functions (diagrams of the models overlap)
Source: [6]

'The 'apparent' time of stabilization of time diagrams – the time after which a model's description is independent from time – for the fractional model is the same as for the classic model.

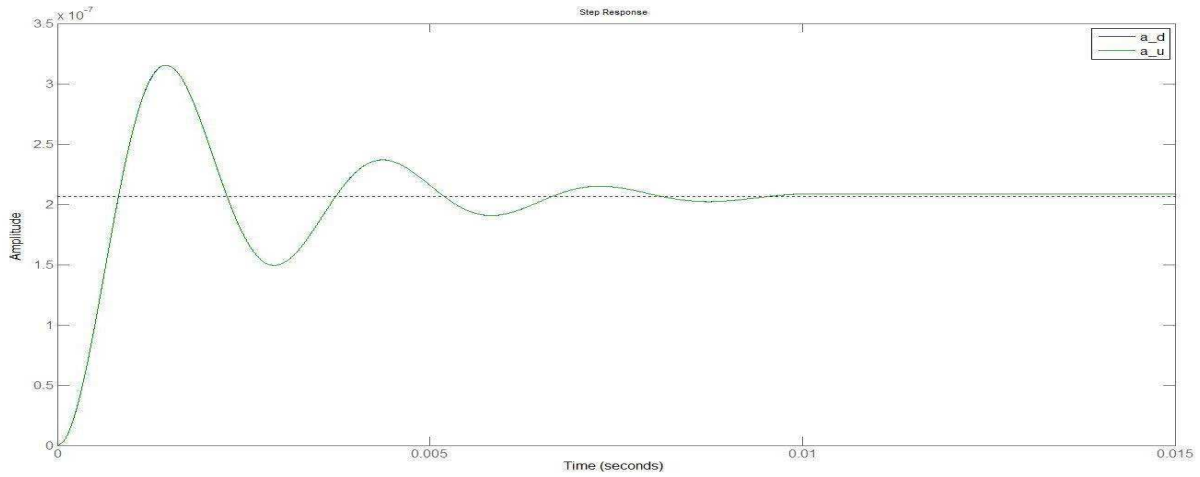

Fig. 8. Comparison of responses by measuring transducer models (11) and (12) to step functions (diagrams of the models overlap)
Source: [6]

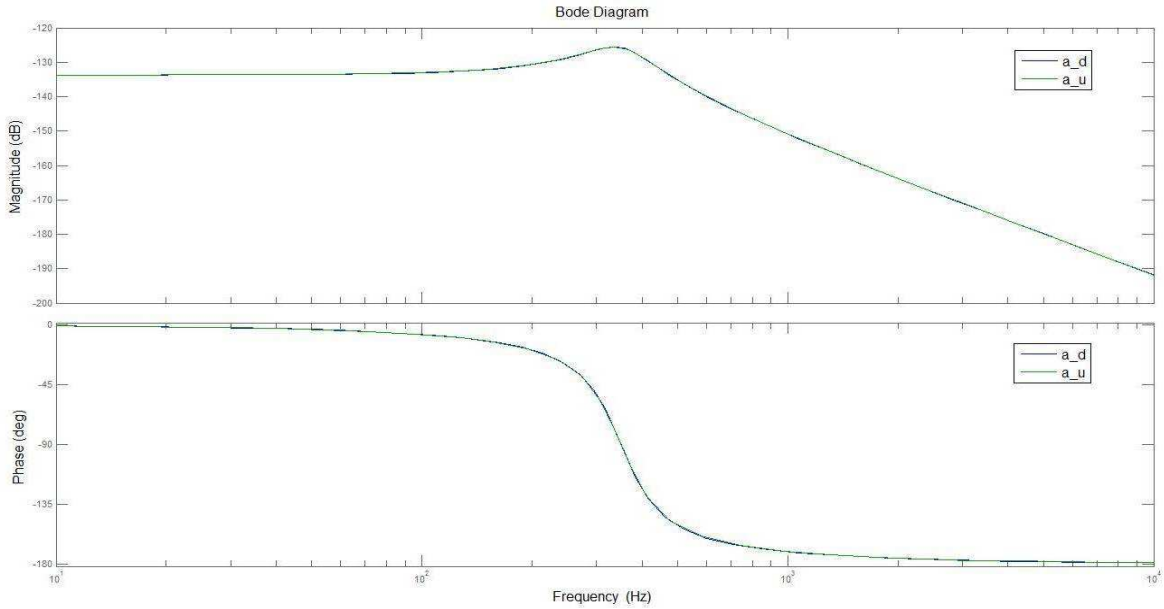

Fig. 9. Comparison of Bode diagrams of measuring transducer models (11) and (12) (diagrams of the models overlap)
Source: [6]

3. MODEL OF A LABORATORY SYSTEM OF ACCELERATION MEASURING TRANSDUCER

Simulation and laboratory testing was undertaken of the accelerometer measurement system. The system was constructed at the Measuring Transducers Laboratory, Department of Measurement Automatics and Engineering, Faculty of Transport and Electrical Engineering of Kazimierz Pulaski University of Technology and Humanities in Radom. An overview of the measurement system is shown in Fig. 10.

In order to determine measuring transducer's operator transmittance, a system comprising two accelerometers (6), (7), conditioner (1) and μDAQ USB-26A16 measurement card (3) was modelled. Accelerometer (7) DeltaTron by Bruel&Kjaer type 4507, sensitivity 10.18mV/ms^{-2} and the range of frequency measurements from 0.4Hz to 6kHz was tested. The conditioner's operating range was between 1Hz and 20kHz. The transducer was mounted on

an electrodynamic inductor (5). A model accelerometer (6) by VEB Metra, type KB12, sensitivity 317mV/ms^{-2} was aligned with the tested transducer.

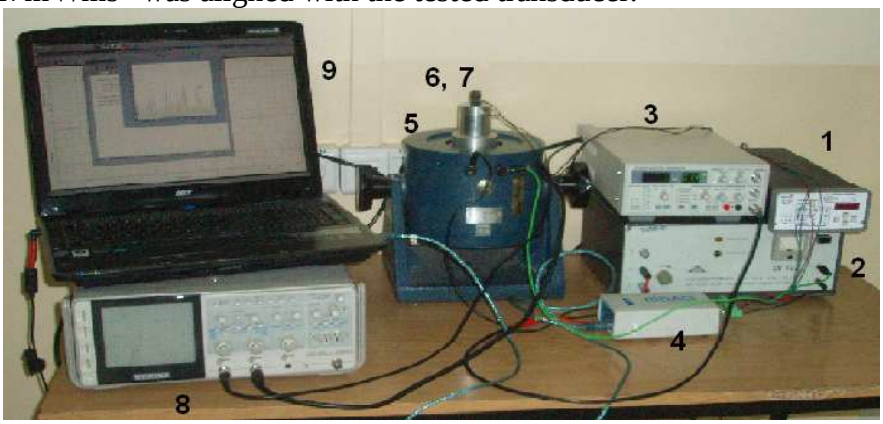

Fig. 10. Laboratory measurement system for testing of mechanical vibration transducers:
1 – conditioner, 2 – generator, 3 – amplifier, 4 – measurement card μDAQ USB-26A16,
5 – inductor, 6, 7 – model and tested measuring transducers, 8 – oscilloscope 9 – computer
Source: [2], [3], [4], [6]

The operator transmittance (15) describing dynamics of the measurement system was determined by identification with an external ARX (AutoRegressive with EXternal input):

$$G(s) = \frac{0.03215s^2 + 1319.6s + 1.338 \cdot 10^6}{s^2 + 4.678 \cdot 10^4 s + 2.309 \cdot 10^7} \tag{15}$$

The voltage signal from the end of the tested measurement track is the identified signal, signal from the model accelerometer in response to the generator's sinusoid function (2) of 100Hz is the comparative signal. ARX identification method produced the operator transmittance $G(s)$ describing the system's dynamics (classic model):

- Discrete transfer function of the model was determined on the basis of the operator transmittance (15):

$$G(s) = \frac{0.03215z^2 - 0.05368z + 0{,}02163}{z^2 + 1.625z + 0.6264} \tag{16}$$

The classic discrete model (16) was produced by discretising the classic model (14) by means of the 'Zero-Order-Hold' method with the sampling time $T_p = 10^{-4}$ s, for which Nyquist theorem of sampling frequency selection obtains.

- Discrete transfer function of fractional models was determined with a method implemented in MATLAB&Simulink. For varying increment of h, quasi-fractional transducer models become discrete transmittances:

$$G_{f_1}(z) = \frac{3.228z^2 - 6.443z + 3.215}{100.5z^2 - 200.5z + 100}, \quad h = 10^{-7} \tag{17a}$$

$$G_{f_2}(z) = \frac{3.347z^2 - 6.562z + 3.215}{104.7z^2 - 204.7z + 100}, \quad h = 10^{-6} \tag{17b}$$

$$G_{f_3}(z) = \frac{4.548z^2 - 7.75z + 3.215}{104.7z^2 - 246.8z + 100}, \quad h = 10^{-5} \tag{17c}$$

$$G_{f_4}(z) = \frac{1.775z^2 - 1.963z + 0.322}{59.09z^2 - 66.78z + 10}, \quad h = 10^{-4} \tag{17d}$$

$$G_{f_5}(z) = \frac{2.69z^2 - 1.384z + 0.032}{70.87z^2 - 48.78z + 1}, \quad h = 10^{-3} \tag{17e}$$

The model of the real measurement system in the form of discrete transmittance and models expressed by means of a differential-integral equation were then compared. Both types of the models were based on the classic model derived by ARX identification method.

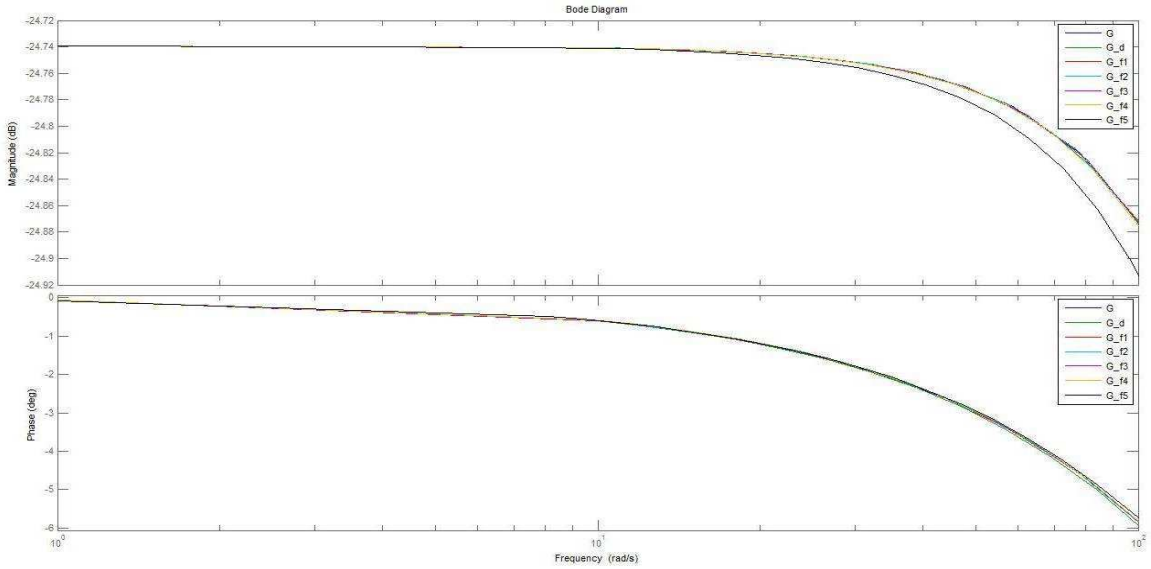

Fig. 11. Bode frequency diagrams of measuring transducer models of transmittance (15) – (17e)
Source: [6]

The simulations were carried out by ode3 integration method for a 100Hz sinusoid input signal. Fig. 11 shows logarithm frequency amplitude and phase diagrams of the measurement system models. It can be observed that, for the adopted increment of h, measure of differentiation accuracy, the diagrams clearly diverge. This means that other h increments, far lower than the sampling frequency, must be adopted.

4. EQUATION OF NON-INTEGRAL ORDER TRANSDUCER DYNAMICS

The Riemann-Liouville's or the Grünwald-Letnikov's definition can be stated for non-integral order derivatives. Let the fractional derivative be:

$$ {}_{t_0}D_t^{(v)} f(t) = \lim_{\substack{h\to 0 \\ t-t_0=kh}} \left[\frac{1}{h^v} \sum_{i=0}^{k} a_i^{(v)} f(t-hi) \right] \tag{18} $$

or:

$$ {}_{t_0}D_t^{(v)} f(t) = \lim_{\substack{h\to 0 \\ t-t_0=kh}} \left[\frac{1}{h^v} \sum_{i=0}^{k} a_i^{(v)} f(t-hi) \right] \begin{bmatrix} f(t) \\ f(t-h) \\ \dots \\ f(t-kh) \end{bmatrix} \tag{19} $$

where:

$$ a_i^{(v)} = \begin{cases} 1 & i = 0 \\ (-1)^i \dfrac{v(v-1)(v-2)\dots(v-i+1)}{i!} & i = 1,2,3,\dots \end{cases} \tag{20} $$

is defined as the reverse difference of the discrete function and h is the increment of $f(t)$ defined in the range $[t_0, t]$:

$$ h = \frac{t-t_0}{k} . \tag{21} $$

Introducing a non-integral order to the measuring transducer's equation (1) we obtain:

$$ \frac{d^2}{dt^2} w(t) + 2\zeta\omega_0 \frac{d}{dt^{(v_1)}} {}^{(v_1)}w(t) + \omega_0^2 w(t) = -\frac{d^2}{dt^2} x(t) \tag{22} $$

Generalising (22) and considering that integral-order derivatives in the derivative-integral

calculus are a special case of non-integral order derivatives, one can formulate:

$$A_2 \frac{d^{(\nu_2)}}{dt^{(\nu_2)}} w(t) + A_1 \frac{d^{(\nu_1)}}{dt^{(\nu_1)}} w(t) + A_0 \frac{d^{(\nu_0)}}{dt^{(\nu_0)}} w(t) = B_2 \frac{d^{(u_2)}}{dt^{(u_2)}} x(t) + B_1 \frac{d^{(u_1)}}{dt^{(u_1)}} x(t) + B_0 \frac{d^{(u_0)}}{dt^{(u_0)}} x(t). \quad (23)$$

where: u, v – non-integral order derivatives.

Let (23) be a linear differential equation of non-integral orders:

$$\sum_{i=0}^{n} t_0 A_i D_{t_0}^{(\nu_i)} w(t) = \sum_{j=0}^{m} t_0 B_j D_{t_0}^{(u_j)} x(t) \quad (24)$$

where:

$A_i = const. \in R,\ i = 1, 2, ..., n-1,\ B_j = const. \in R,$

$j = 1, 2, ..., m,\ m \le n,\ m, n \in R,\ A_n = 1,$

$t_0 A_i D_{t_0}^{(\nu_i)} w(t)$, $t_0 B_j D_{t_0}^{(u_j)} x(t)$ – Riemann-Liouville's or Grünwald-Letnikov's derivatives,

$t_0 A_i D_{t_0}^{(\nu_i)} w(t)\Big|_{t=t_0}$, $t_0 B_j D_{t_0}^{(u_j)} x(t)\Big|_{t=t_0}$ – initial conditions,

$w(t)$, $x(t)$ – functions for which Riemann-Liouville's or Grünwald-Letnikov's derivatives exist.

Taking (24) into account, (23) can be expressed as:

$$\begin{bmatrix} A_2 & A_1 & A_0 \end{bmatrix} \begin{bmatrix} D_t^{(\nu_2)} w(t) \\ D_t^{(\nu_1)} w(t) \\ D_t^{(\nu_0)} w(t) \end{bmatrix} = \begin{bmatrix} B_2 & B_1 & B_0 \end{bmatrix} \begin{bmatrix} D_t^{(u_2)} x(t) \\ D_t^{(u_1)} x(t) \\ D_t^{(u_0)} x(t) \end{bmatrix}. \quad (25)$$

Introducing factors $a_2^{\nu_i}, a_1^{\nu_i}, a_0^{\nu_i}$ and $b_2^{u_j}, b_1^{u_j}, b_0^{u_j}$ to (25), with: $a_0^{(\nu_i)} = 1$ for $i = 1, 2, ..., n$, $b_0^{(u_j)} = 1$ for $j = 1, 2, ..., m$ and: $a_0 = \frac{A_n}{h^{\nu_n}} + \frac{A_{n-1}}{h^{\nu_{n-1}}} + ... + \frac{A_0}{h^{\nu_0}}$, $b_0 = \frac{A_m}{h^{u_m}} + \frac{A_{m-1}}{h^{u_{m-1}}} + ... + \frac{A_0}{h^{u_0}}$.

Considering:

$$\begin{bmatrix} D_t^{(\nu_2)} w(t) \\ D_t^{(\nu_1)} w(t) \\ D_t^{(\nu_0)} w(t) \end{bmatrix} = \begin{bmatrix} \frac{1}{h^{\nu_2}} & 0 & 0 \\ 0 & \frac{1}{h^{\nu_1}} & 0 \\ 0 & 0 & \frac{1}{h^{\nu_0}} \end{bmatrix} \begin{bmatrix} a_0^{(\nu_2)} & a_1^{(\nu_2)} & a_2^{(\nu_2)} \\ a_0^{(\nu_1)} & a_1^{(\nu_1)} & a_2^{(\nu_1)} \\ a_0^{(\nu_0)} & a_1^{(\nu_0)} & a_2^{(\nu_0)} \end{bmatrix} \begin{bmatrix} w(2h) \\ w(h) \\ w(0h) \end{bmatrix} \quad (26)$$

and:

$$\begin{bmatrix} D_t^{(u_2)} x(t) \\ D_t^{(u_1)} x(t) \\ D_t^{(u_0)} x(t) \end{bmatrix} = \begin{bmatrix} \frac{1}{h^{u_2}} & 0 & 0 \\ 0 & \frac{1}{h^{u_1}} & 0 \\ 0 & 0 & \frac{1}{h^{u_0}} \end{bmatrix} \begin{bmatrix} b_0^{(u_2)} & b_1^{(u_2)} & b_2^{(u_2)} \\ b_0^{(u_1)} & b_1^{(u_1)} & b_2^{(u_1)} \\ b_0^{(u_0)} & b_1^{(u_0)} & b_2^{(u_0)} \end{bmatrix} \begin{bmatrix} x(2h) \\ x(h) \\ x(0h) \end{bmatrix} \quad (27)$$

produces the following matrix equation:

$$\begin{bmatrix} A_2 & A_1 & A_0 \end{bmatrix} \begin{bmatrix} \frac{1}{h^{\nu_2}} & 0 & 0 \\ 0 & \frac{1}{h^{\nu_1}} & 0 \\ 0 & 0 & \frac{1}{h^{\nu_0}} \end{bmatrix} \begin{bmatrix} a_0^{(\nu_2)} & a_1^{(\nu_2)} & a_2^{(\nu_2)} \\ a_0^{(\nu_1)} & a_1^{(\nu_1)} & a_2^{(\nu_1)} \\ a_0^{(\nu_0)} & a_1^{(\nu_0)} & a_2^{(\nu_0)} \end{bmatrix} \begin{bmatrix} w(2h) \\ w(h) \\ w(0h) \end{bmatrix} = \begin{bmatrix} a_2 & a_1 & a_0 \end{bmatrix} \begin{bmatrix} w(2h) \\ w(h) \\ w(0h) \end{bmatrix} \quad (28)$$

and:

$$\left[B_2\frac{1}{h^{u_2}}\quad B_1\frac{1}{h^{u_1}}\quad B_0\frac{1}{h^{u_0}}\right]\begin{bmatrix}b_0^{(u_2)} & b_1^{(u_2)} & b_2^{(u_2)}\\ b_0^{(u_1)} & b_1^{(u_1)} & b_2^{(u_1)}\\ b_0^{(u_0)} & b_1^{(u_0)} & b_2^{(u_0)}\end{bmatrix}\begin{bmatrix}x(2h)\\ x(h)\\ x(0h)\end{bmatrix}=\begin{bmatrix}b_2 & b_1 & b_0\end{bmatrix}\begin{bmatrix}x(2h)\\ x(h)\\ x(0h)\end{bmatrix} \tag{29}$$

where:

$$\left[A_2\frac{1}{h^{v_2}}\quad A_1\frac{1}{h^{v_1}}\quad A_0\frac{1}{h^{v_0}}\right]\begin{bmatrix}a_0^{(v_2)} & a_1^{(v_2)} & a_2^{(v_2)}\\ a_0^{(v_1)} & a_1^{(v_1)} & a_2^{(v_1)}\\ a_0^{(v_0)} & a_1^{(v_0)} & a_2^{(v_0)}\end{bmatrix}=\begin{bmatrix}a_2 & a_1 & a_0\end{bmatrix} \tag{30}$$

and:

$$\left[B_2\frac{1}{h^{u_2}}\quad B_1\frac{1}{h^{u_1}}\quad B_0\frac{1}{h^{u_0}}\right]\begin{bmatrix}b_0^{(u_2)} & b_1^{(u_2)} & b_2^{(u_2)}\\ b_0^{(u_1)} & b_1^{(u_1)} & b_2^{(u_1)}\\ b_0^{(u_0)} & b_1^{(u_0)} & b_2^{(u_0)}\end{bmatrix}=\begin{bmatrix}b_2 & b_1 & b_0\end{bmatrix}\cdot \tag{31}$$

Equation (25) finally becomes:

$$\begin{bmatrix}a_2 & a_1 & a_0\end{bmatrix}\begin{bmatrix}w(2h)\\ w(h)\\ w(0h)\end{bmatrix}=\begin{bmatrix}b_2 & b_1 & b_0\end{bmatrix}\begin{bmatrix}x(2h)\\ x(h)\\ x(0h)\end{bmatrix}. \tag{32}$$

Method of reducing the differential equation (23) to the matrix equation (32) was verified by determining logarithm frequency diagrams of elementary terms (Fig. 12.) and of transducers for the adopted non-integral orders in (23) (Fig. 13) and obtaining the desired diagram courses (overlapping of the diagrams). The diagrams can be observed to clearly overlap for all the adopted h increments. This means that h increments far lower than the sampling frequency should be assumed.

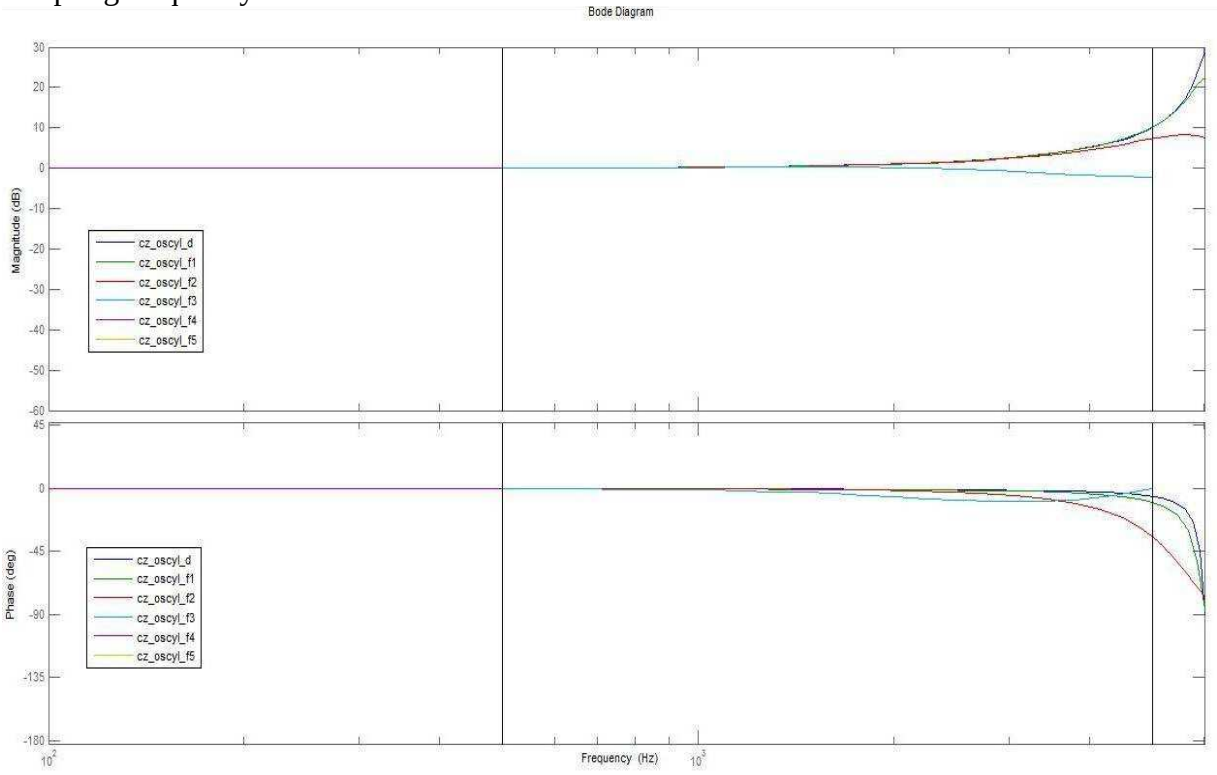

Fig. 12. Frequency Bode diagrams of the integral and non-integral order oscillatory term:
cz_oscyl_d – integral-order oscillatory term
Source: [6]

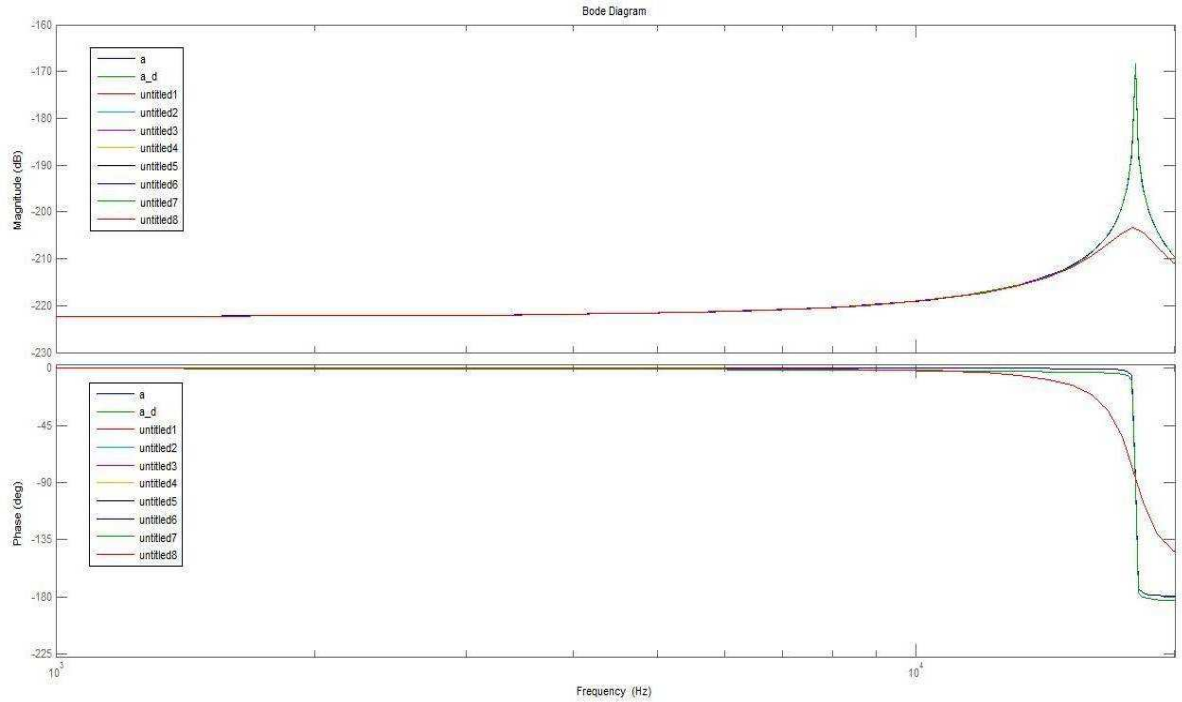

Fig. 13. Logarithm frequency Bode diagrams of the transducer model for v_1=1.8 and successive v_2 orders, from 1.4 to 2.8
Source: [6]

The results of the work proposed within the framework of this paper are to answer the questions related to legitimacy of modelling dynamic properties of accelerometers by means of fractional order differential equations, and in particular to answer the basic question: *"Is abandoning the classical modelling of dynamic properties by means of integer order differential equations in favour of fractional order ones justified from the point of view of accuracy of dynamic behaviour modelling?"* Due to scarcity of literature on the topic of using fractional order differential equations for modelling accelerometers (and generally measuring sensors), the paper proposed is a pioneering one.

The results obtained, though mainly concerning the research into modelling of the accelerometer dynamic behaviour, will be relevant for modelling dynamic properties of a very wide group of sensors and measuring transducers due to the typical notation of dynamic behaviour in a form of differential equations. As this way of modelling is commonly accepted, not only for modelling objects but also phenomena, it is assumed that the research results obtained within the framework of this project will be significant for the discussions about a general and common application of fractional calculus for modelling physical phenomena.

CONCLUSIONS

The comparison of classic and fractional models responses to the step function implies the time after which diagrams stabilise for fractional models is the same as for the classic model. The same applies to frequency diagrams for fractional discrete models, which have the same course in the tested frequency ranges as the classic models. This means that non-integral order differential-integral calculus is a generalisation of integral-order differential calculus – this is confirmed by laboratory testing of dynamic systems.

In order to verify the method of developing a transducer equation for non-integral orders, forms of elementary term diagrams determined by means of this method were tested – the oscillatory term was selected, which has the same differential expression as the accelerometer.

Effect of h increment variations on fractional measuring transducer's amplitude and phase diagrams has also been shown in this paper.

Application of the alternative, generalised method of describing dynamic properties of measuring transducers discussed in this article, based on non-integral order differential-integral calculus, will help to undertake analyses of simulated dynamics of various objects and processes which, due to their complexity, must be described by means of differential equations of any orders. This method appears to enhance accuracy of simulations compared to current methods not only for elements like the measuring transducer covered in this article but also for systems comprising a number of devices or complex physical phenomena.

REFERENCES

1. Kaczorek T.: *Selected Problems of Fractional Systems Theory*, Springer-Verlag GmbH, 344 pages, ISBN 978-3-642-20501-9, Berlin, Germany 2011.
2. Luft M., Cioć R., Pietruszczak D.: *Examples of the fractional calculus application in control theory and metrology*, CENTRAL EUROPEAN SCHOOL OF DOCTORAL STUDY (CESDS), 20-22.9.2011, Trenčianske Teplice, Slovak Republic, pp. 65-69, ISBN 978-80-554-0421-9, Published by University of Zilina, Slovak Republic 2011.
3. Luft M., Cioć R., Pietruszczak D.: *Fractional calculus in modelling of measuring transducers*, ELECTRONICS AND ELECTRICAL ENGINEERING, Nr. 4(110), ISSN 1392-1215 (print), ISSN 2029-5731 (online), Kaunas, Lithuania 2011.
4. Luft M., Łukasik Z., Szychta E., Cioć R., Pietruszczak D.: *Selected issues of fractional calculus in mathematical modelling of measuring transducers used in transportation facilities*, EXPLO-SHIP 2012, 15-17.05, Świnoujście 2012.
5. Ostalczyk P.: *Zarys rachunku różniczkowo-całkowego ułamkowych rzędów. Teoria i zastosowanie w automatyce (Epitome of the fractional calculus. Theory and its applications in automatic)*, Wydawnictwo Politechniki Łódzkiej, stron 430, ISBN 978-83-7283-245-0, Łódź 2008. (*published in Polish*)
6. Pietruszczak D.: *Analiza właściwości układów pomiarowych wielkości dynamicznych z wykorzystaniem rachunku różniczkowo-całkowego ułamkowych rzędów (Application of fractional calculus to the analysis of dynamic properties of the measurement systems)*, Doctoral dissertation, The Main Library of Kazimierz Pulaski University of Technology and Humanities in Radom, Radom 2012. (*published in Polish*)

BADANIA LABORATORYJNE WŁAŚCIWOŚCI DYNAMICZNYCH AKCELEROMETRÓW NIECAŁKOWITYCH RZĘDÓW

Streszczenie

W artykule przedstawiono możliwości zastosowania rachunku różniczkowo-całkowego niecałkowitych rzędów w miernictwie dynamicznym. Przedstawiono układ pomiarowy do badań właściwości dynamicznych akcelerometrów W procesie identyfikacji przetwornika pomiarowego zastosowano metodę ARX. Porównano właściwości dynamiczne przetwornika pomiarowego całkowitego i niecałkowitego rzędu. Wskazano na zalety zastosowania rachunku różniczkowo-całkowego niecałkowitych rzędów do opisu dynamiki przetworników pomiarowych.

***Autorzy**:*

Prof. dr hab. inż. **Mirosław LUFT** – Uniwersytet Technologiczno-Humanistyczny im. Kazimierza Pułaskiego w Radomiu, Wydział Transportu i Elektrotechniki, ul. Malczewskiego 29, 26-600 Radom, m.luft@uthrad.pl

Dr hab. inż. **Elżbieta SZYCHTA**, prof. UTH Rad. – Uniwersytet Technologiczno-Humanistyczny im. Kazimierza Pułaskiego w Radomiu, Wydział Transportu i Elektrotechniki, ul. Malczewskiego 29, 26-600 Radom, e.szychta@uthrad.pl

Dr inż. **Daniel PIETRUSZCZAK** – Uniwersytet Technologiczno-Humanistyczny im. Kazimierza Pułaskiego w Radomiu, Wydział Transportu i Elektrotechniki, ul. Malczewskiego 29, 26-600 Radom, d.pietruszczak@uthrad.pl